1

Topological Order and Quantum Criticality

Claudio Castelnovo
Rudolf Peierls Centre for Theoretical Physics and Worcester College, Oxford University, Oxford OX1 3NP, UK

Simon Trebst
Microsoft Research, Station Q, University of California, Santa Barbara, California 93106, USA

Matthias Troyer
Theoretische Physik, Eidgenössische Technische Hochschule Zurich, 8093 Zurich, Switzerland

In this chapter we discuss aspects of the quantum critical behavior that occurs at a quantum phase transition separating a topological phase from a conventional one. We concentrate on a family of quantum lattice models, namely certain deformations of the toric code model, that exhibit continuous quantum phase transitions. One such deformation leads to a Lorentz-invariant transition in the 3D Ising universality class. An alternative deformation gives rise to a so-called conformal quantum critical point where equal-time correlations become conformally invariant and can be related to those of the 2D Ising model. We study the behavior of several physical observables, such as non-local operators and entanglement entropies, that can be used to characterize these quantum phase transitions. Finally, we briefly consider the role of thermal fluctuations and related phase transitions, before closing with a short overview of field theoretical descriptions of these quantum critical points.

1.1 Introduction

Topological phases are distinct both from high-temperature disordered phases and conventional ordered ones: they exhibit order, albeit of a type which cannot be defined locally [1]. They are often described by an emergent symmetry that is captured by a new set of quantum numbers such as a ground-state

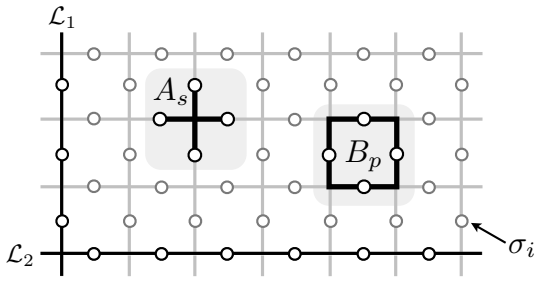

FIGURE 1.1
The toric code model: The elementary degrees of freedom are SU(2) spin-1/2's on the bonds of a square lattice. The star operator A_s acts on the spins surrounding a vertex and the plaquette operator B_p acts on the spins surrounding a plaquette.

degeneracy and fractional quasiparticle statistics. The archetypal physical realizations of topologically ordered states are fractional quantum Hall states.

This chapter is concerned with topological order and quantum critical behavior in the context of microscopic lattice models. Most of our discussion will concentrate on *time-reversal invariant* systems which in more general terms can be described by so-called quantum double models and are thus quite distinct from fractional quantum Hall states. We start by shortly reviewing the *toric code* model, a particularly simple and exactly solvable spin-1/2 model that exhibits an Abelian topological phase. Our subsequent discussion of quantum phase transitions involving topologically ordered phases of matter is structured around two types of deformations of the toric code which we dub "Hamiltonian deformation" and "wavefunction deformation", respectively, and that give rise to distinct quantum critical points. We then turn to finite-temperature phase transitions and discuss under which circumstances topological order is robust with regard to thermal fluctuations.

1.1.1 The toric code

The toric code (TC) [2] is an exactly solvable model of SU(2) spin-1/2 degrees of freedom, which is typically defined on a square lattice, but can be adapted to other two-dimensional lattice geometries (and even higher-dimensional lattices). The Hamiltonian is generally defined as a sum of vertex and plaquette terms

$$\mathcal{H}_{\mathrm{TC}} = -J_e \sum_s A_s - J_m \sum_p B_p \,, \tag{1.1}$$

where the star operator A_s acts on all spins adjacent to a vertex s by coupling their σ^x spin components, $A_s = \prod_{j \in \mathrm{star}(s)} \sigma_j^x$, and the plaquette operator B_p acts on all spins surrounding a plaquette p by coupling their σ^z spin

components, $B_p = \prod_{j\in\partial p} \sigma_j^z$. We typically consider the case $J_e, J_m > 0$. In the case of the square lattice, the star and plaquette operators are both 4-spin operators which are Hermitian and have eigenvalues ± 1.

The toric code model can be solved exactly, since all terms in the Hamiltonian commute with one another. Indeed, $A_s B_p = B_p A_s$, $\forall\, s, p$ since any given pair of vertex and plaquette operators either share 0 or 2 bonds, and thus all minus signs arising from the commutation of σ^x and σ^z on those bonds cancel. This allows to construct eigenstates $|\xi\rangle$ of the toric code as common eigenstates of all terms in the Hamiltonian. For a ground state the minimization of the energy then gives the "stabilizer conditions" $A_s |\xi\rangle = B_p |\xi\rangle = |\xi\rangle$ for each vertex/plaquette term, and an overall ground-state energy $E_0 = -N(J_e + J_m)$, where N is the number of sites on the lattice.

For a square lattice with periodic boundary conditions in both space directions (thus forming a torus) the sign of the vertex (plaquette) terms can only be flipped on an *even* number of vertices (plaquettes). This implies that there are two overall constraints

$$\prod_s A_s = \prod_p B_p = +1\,.$$

This in turn lets us estimate the ground-state degeneracy on a torus: The total Hilbert space has 2^{2N} states. With the above constraint there are only $2N-2$ independent choices of the A_s and B_p operators, thus imposing 2^{2N-2} conditions. As a consequence, we have $2^{2N}/2^{2N-2} = 4$ ground states on the torus.

Another way to see how this ground-state degeneracy arises is by explicitly constructing the ground-state wavefunctions. In doing so we solve the toric code Hamiltonian in the σ^z basis and introduce classical variables $z_j = \pm 1$ to label the σ^z basis states. This allows to define a plaquette flux

$$\phi_p(\mathbf{s}) = \prod_{j\in\partial p} z_j$$

for each classical spin configuration $\mathbf{s} = \{z_j\}_{j=1}^{2N}$. If $\phi_p = -1$, we say there is a vortex on plaquette p. For a ground state $|\psi\rangle$ of the toric code we need to maximize each plaquette term $B_p |\psi\rangle = |\psi\rangle$ and thus find that a ground state contains no vortices

$$|\psi\rangle = \sum_{\{\mathbf{s}\,:\,\phi_p(\mathbf{s})=+1\ \forall p\}} c_{\mathbf{s}} |\mathbf{s}\rangle\ .$$

To maximize the vertex operator, e.g. $A_s |\psi\rangle = |\psi\rangle$, all coefficients $c_{\mathbf{s}}$ are then required to be equal (for each orbit of the action of the star operators). A ground state of the toric code is thus an equal-weight superposition of vortex-free spin configurations.

On the square lattice there are four distinct ways to construct such equal-weight superpositions, giving rise to a four-fold ground-state degeneracy. This

can be seen by considering the following function measuring the flux through an extended loop $\mathcal{L}$ (similar to a Wilson loop), as indicated in Fig. 1.1

$$\Phi_{\mathcal{L}}(\mathbf{s}) = \prod_{j \in \mathcal{L}} z_j \,.$$

If the loop $\mathcal{L}$ is a contractible loop, then the flux $\Phi_{\mathcal{L}}$ is simply the product of the plaquette fluxes ϕ_p within the loop (reminiscent of Stoke's theorem), and for each ground state $\Phi_{\mathcal{L}} = +1$. If on the other hand the loop $\mathcal{L}$ is an essential loop on the torus (which cannot be contracted), then the flux $\Phi_{\mathcal{L}} = \pm 1$ defines a conserved quantity, since an arbitrary star operator A_s overlaps with the loop $\mathcal{L}$ in either 0 or 2 bonds and thus preserves $\Phi_{\mathcal{L}}$. For the torus there are two independent, essential loops $\mathcal{L}_1$, $\mathcal{L}_2$ wrapping the torus as illustrated in Fig. 1.1. The ground states of the toric code can then be labeled by two conserved quantities $\Phi_{\mathcal{L}_1} = \pm 1$ and $\Phi_{\mathcal{L}_2} = \pm 1$. The resulting degeneracy originates from the four distinct *topological sectors* defined by the essential loops. Embedding the toric code onto the surface of a more general manifold, one finds that the ground-state degeneracy increases as 4^g with the genus g of the underlying surface.

We note in passing that one can find another description of the eigenstates of the toric code by solving the Hamiltonian in the σ^x basis. Labeling the basis states by classical variables $x_j = \pm 1$ and identifying the $x_j = +1$ states with loop segments on the corresponding bonds, one finds that the ground states of the toric code form a *quantum loop gas* with fugacity $d = 1$. The four topological sectors then correspond to loop configurations with an even or odd number of loops wrapping the torus across two independent, non-contractible cuts.

The toric code Hamiltonian can also be viewed as a particular lattice regularization of an Ising gauge theory [3]. In this language the spins residing on the bonds correspond to Z_2 valued gauge potentials, the star operators A_s become gauge transformations, and their commutation with the plaquette flux operators B_p implies an overall gauge invariance. Owing to this equivalence to an Ising gauge theory, the two distinct excitations of the toric code that arise from violating one of the stabilizer conditions of the ground states, $A_s \,|\psi\rangle = |\psi\rangle$ and $B_p \,|\psi\rangle = |\psi\rangle$, are commonly identified as *electric charges* and *magnetic vortices*, respectively.

For a given ground state a pair of electric charges is created by applying the σ^z-operator to a spin, which leads to a violation of the stabilizer condition $A_s \,|\psi\rangle = |\psi\rangle$ on the two adjacent vertices. Therefore, the energy cost to create two electric charges is $4J_e$. While a pair of electric charges does not need to reside on neighboring vertices, it remains connected for any separation by an electric path operator $\prod_{j \in \ell} \sigma_j^z$, where ℓ is a path connecting the two vertices. Similarly for a pair of magnetic vortices, upon replacing ℓ with a path on the dual lattice.

Both types of excitations are massive quasiparticles, and for the unperturbed toric code Hamiltonian (1.1) they are static excitations which do not

disperse. While single electric charges or magnetic vortices are bosons (considering the exchange with the same particle type), the composite quasiparticle of an electric charge plus a magnetic vortex constitutes a fermion. Moreover, electric charges and magnetic vortices exhibit an unusual, *mutual* exchange statistics in that they are mutual *semions* – the simplest incarnation of Abelian anyons: when moving an electric charge around a magnetic vortex the wavefunction picks up a phase of $e^{i\pi} = -1$. This can best be seen when considering a wavefunction $|\xi\rangle$ of a state containing a single vortex at a plaquette $\tilde{p}$, e.g. $B_{\tilde{p}}\,|\xi\rangle = -\,|\xi\rangle$. If we move an electric charge along a contractible loop $\mathcal{L}$ around this plaquette $\tilde{p}$, the wavefunction transforms as

$$|\xi\rangle \;\rightarrow\; \prod_{j\in\mathcal{L}} \sigma_j^z\,|\xi\rangle \;=\; \prod_{p \text{ inside } \mathcal{L}} B_p\,|\xi\rangle = -\,|\xi\rangle \;,$$

which reveals the mutual semionic statistics.

In summary, the toric code is one of the simplest and most accessible quantum lattice models that gives rise to a quantum state with *topological order*. This exotic quantum order reveals itself in a (robust) ground-state degeneracy, and massive, deconfined quasiparticles with mutual anyonic statistics.

1.2 Quantum Phase Transitions

While conventional ordered phases arise from the spontaneous breaking of a symmetry, the converse is true for topological phases which exhibit an enhanced symmetry at low energies. It is this emerging topological invariance which isolates the low-energy degrees of freedom from local perturbations and gives rise to stable topological phases. However, even a local perturbation, if sufficiently strong, can eventually destabilize a topological phase and give rise to a quantum phase transition.

To elucidate the quantum critical behavior at such a transition we consider the pedagogical example of the toric code in a magnetic field. A sufficiently large magnetic field aligns all the spins with the field resulting in a paramagnetically ordered state, and thus destroys any topological order. The quantum phase transition that connects these two phases can be either first-order or continuous depending on the way we couple the magnetic field to the local spin degrees of freedom in the toric code Hamiltonian. We mostly focus on the latter case of a continuous transition and discuss two distinct types of quantum critical points that can occur.

First, we consider a magnetic field term $\vec{h}\cdot\vec{\sigma}$, where the magnetic field $\vec{h}$ has no tranverse h_y component [4, 5, 6], i.e., $\vec{h}\cdot\vec{\sigma} = h_x\sigma^x + h_z\sigma^z$. This "Hamiltonian deformation" gives rise to a quantum critical point at which the system becomes scale invariant and *local* two-point correlation functions show

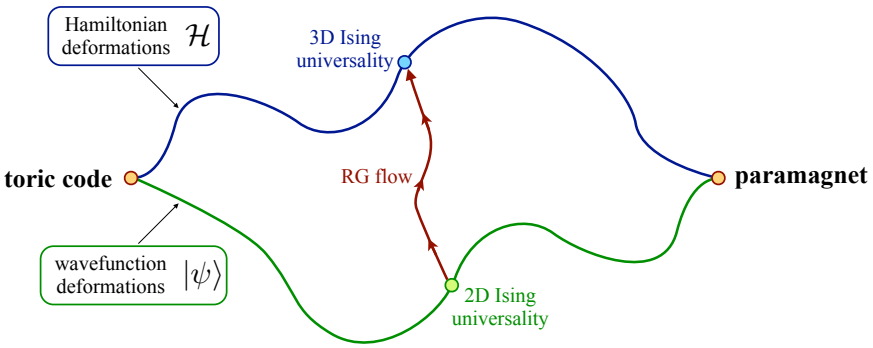

FIGURE 1.2
Toric code deformations: Two distinct types of quantum critical points are observed in phase space depending on the way the magnetic field is coupled to the local spin degrees of freedom in the toric code.

a divergent behavior. This not only allows us to define a dynamical critical exponent, which is found to be $z = 1$, but also enables us to characterize this Lorentz-invariant transition out of the topological phase in terms of a conventional universality class, which for this transition turns out to be the classical 3D Ising model.

Second, we consider a magnetic field term $\exp(-h_z\sigma^z)$, which for large field strength projects onto the fully polarized state, while allowing to keep track of the ground-state wavefunction for all field strengths [7, 8]. We call this second scenario a "wavefunction deformation". It gives rise to a so-called *conformal quantum critical point* [9], where a peculiar type of dimensionality reduction is at play which allows to describe the equal-time correlations of the ground state by a 2+0 dimensional conformal field theory which at this quantum critical point turns out to be the 2D Ising theory. In contrast to the "Hamiltonian deformation" the dynamical critical exponent is $z \neq 1$ for this second quantum critical point. Despite the obvious differences in the intermediate quantum critical behavior both "deformations" connect the same extremal ground states, namely those of the toric code with a fully polarized, paramagnetic state.

We note in passing that (in the continuum limit) these two quantum critical points are connected by a renormalization group flow from the conformal quantum critical point to the Lorentz-invariant quantum critical point. A schematic overview of these two types of deformations and their respective quantum critical points is given in Fig. 1.2.

Finally, we close by discussing the role of thermal fluctuations at the quantum critical points of the deformed toric code models. This also allows to shed some light on the question whether topological order can survive up to a finite temperature.

1.2.1 Lorentz-invariant transitions

We first turn to the case of Lorentz-invariant quantum critical points which can be observed when adding a longitudinal magnetic field to the toric code

$$\mathcal{H}_{\mathrm{TC+LMF}} = -J_e \sum_s A_s - J_m \sum_p B_p + \sum_i \left(h_x \sigma_i^x + h_z \sigma_i^z\right) . \tag{1.2}$$

Whereas the model is no longer exactly solvable, we can readily understand the extremal cases of weak and strong magnetic fields.

For $h_z = 0$ the effect of a small field $h_x \ll J_e, J_m$ is the virtual creation and annihilation of pairs of magnetic vortices as discussed in the previous section, or the hopping of a vortex excitation by one plaquette which allows the vortices to acquire a dispersion. In first-order perturbation theory this gives the usual tight-binding form in momentum space

$$E(q_x, q_y) = 2J_m - 2h_x \left(\cos q_x + \cos q_y\right) + O(h_x^2) ,$$

which can be further expanded to higher orders [6]. A similar observation holds for the dual charge excitations.

With increasing magnetic field strength the quasiparticle gap eventually closes and the transition into the paramagnetic state can be understood as the Bose condensation of these quasiparticles. In the language of the Ising gauge theory this leaves us with two seemingly distinct possibilities, as first discussed by Fradkin and Shenker [10]: A Higgs transition into a "charge condensate" with concurrent vortex confinement for $h_x \ll h_z \approx J_e, J_m$, or by duality a confinement transition of the electric charges with the concurrent formation of a "vortex condensate" for $h_z \ll h_x \approx J_e, J_m$. Both transitions gives rise to a *line of continuous transitions*, as illustrated schematically in Fig. 1.3, where fluctuations of the system can be described in terms of two complimentary Z_2 order parameters, namely the amplitudes of the corresponding charge and vortex condensates. As such the two transitions are clearly distinct and owing to the non-trivial mutual statistics of charges and vortices, these two lines of continuous transitions are not expected to join smoothly in the phase diagram. On the basis of extensive numerical simulations it has recently been conjectured [5, 6] that they meet at a *multicritical* point where they join with a first-order line separating the charge and vortex condensates for intermediate $h_x = h_z \approx J_e, J_m$. This first-order transition is accompanied by a sudden change in the density of charges/vortices, similar to a liquid-gas transition. However, if we consider the paramagnetic phase in the large magnetic field limit of the original spin model, then we can continuously rotate the magnetic field in the (h_x, h_z)-plane without inducing a phase transition. As a consequence, the charge and vortex condensates are actually the same phase, and they are connected in the large magnetic field limit. Indeed, the first-order line has a critical endpoint whose location has recently been determined by numerical simulations [5, 6].

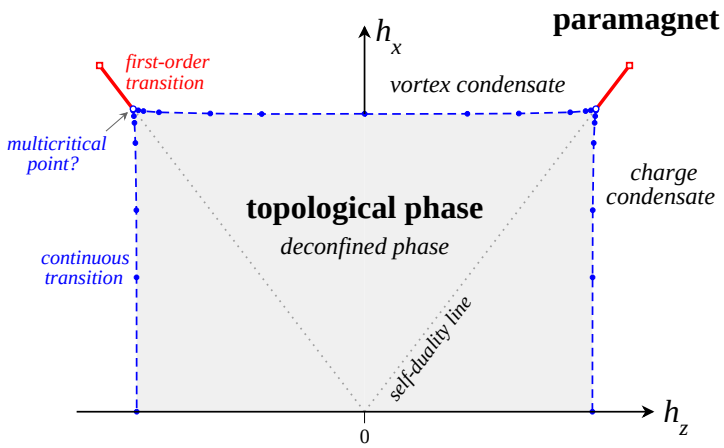

FIGURE 1.3
Phase diagram of the toric code in a longitudinal magnetic field: The dashed lines indicate continuous quantum phase transitions from the topological phase (shaded area) to a paramagnetically ordered state. The solid lines indicate first-order transitions. The figure has been adapted from the numerical data of Ref. [5] for the closely related classical, anisotropic Z_2 gauge Higgs model on a cubic lattice.

To discuss the quantum critical behavior at one of the continuous transitions in the phase diagram of Fig. 1.3 in more detail, we consider the case of a single-component magnetic field in the x-direction, $h_x \neq 0$ and $h_{y,z} = 0$. As discussed before such a magnetic field will create/annihilate virtual vortex pairs that can hop through the lattice, while charge excitations remain gapped and static. To describe the vortex dynamics in this limit we introduce a plaquette spin operator μ_p with eigenvalues $\mu_p^z = \pm 1/2$ depending on the eigenvalue of the plaquette operator B_p on the respective plaquette, e.g. $B_p = 2\mu_p^z$. We can then rewrite the spin operators σ^x in terms of these plaquette operators as $\sigma_i^x = \mu_p^x \mu_q^x$, where p and q are the plaquettes separated by the bond i. With these transformations in place, we can now recast the charge-free low-energy sector of the toric code in a single-component magnetic field in the form

$$\tilde{\mathcal{H}}_{\mathrm{TC+LMF}} = -2J_m \sum_p \mu_p^z + h_x \sum_{\langle p,q \rangle} \mu_p^x \mu_q^x \tag{1.3}$$

of the transverse field Ising model. Its well-known quantum phase transition thus describes the transition from the topological phase of the toric code into a paramagnetic state (or vortex condensate in the language of the Ising gauge theory). This continuous transition in the 3D Ising universality class occurs for coupling strength $(h_x/J_m)_c \approx 0.65692(2)$ [11], indicating that the topological phase is remarkably stable – it takes an $O(1)$ perturbation (in terms of the

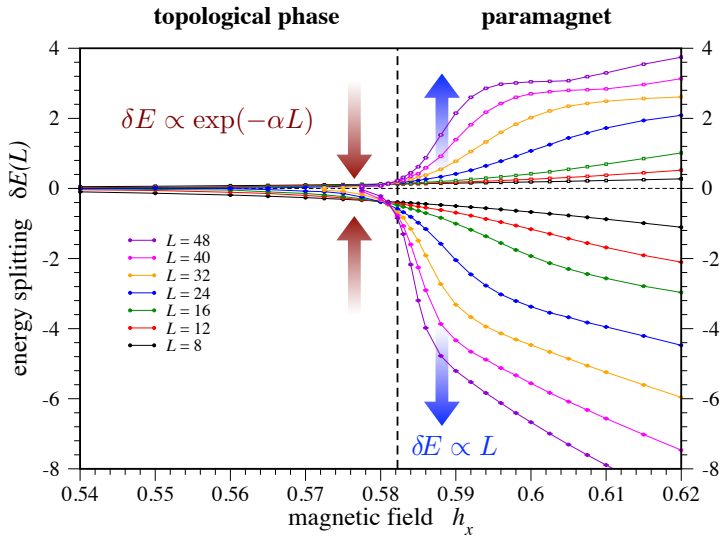

FIGURE 1.4
Splitting of the topological degeneracy: The finite-size splitting of the ground-state degeneracy changes from exponential suppression in the topological phase to linear splitting in the paramagnetic phase. Data for different linear system sizes L are plotted. (The critical coupling is slightly lower than stated in the text, as the numerical simulations were done for discretized imaginary time and isotropic couplings in space-time.)

coupling strengths) to destroy the topologically ordered state, similar to the case of many conventionally ordered states.

The mapping to the transverse field Ising model also allows to perform extensive Monte Carlo simulations of this transition, and to keep track of the ground-state degeneracy across the quantum phase transition [4]. As shown in Fig. 1.4 the finite-size splitting of the degeneracy changes from exponentially small in the topological phase to power-law in the paramagnetic phase (as a function of the linear system size L).

Returning to the full Hamiltonian (1.2) we can ask what effect a small magnetic field h_z has on the quantum phase transition discussed above. Since such a field primarily induces dynamics in the gapped charge sector, the transition into the vortex condensate remains largely untouched, and we expect to observe a *line* of continuous transitions emanating from the single-component field limit discussed above. In fact, one can map out the full phase diagram of the two-component case as shown in Fig. 1.3. This is done through a sequence of transformations that allow to recast the toric code in a two-component magnetic field onto a classical, anisotropic Z_2 gauge Higgs model on a three-dimensional cubic lattice, as described in detail in Ref. [5].

1.2.1.1 Other Hamiltonian deformations

A number of other Hamiltonian deformations of the toric code have been considered in the literature. Of particular interest is the case of a transverse field $h_y\sigma^y$. Contrary to the longitudinal case, it is found to drive a first-order phase transition into a paramagnetic state [12].

The effect of dissipation was also studied [4] by coupling the toric code to an Ohmic heat bath. A Thouless-type phase transition was found when the bath couples to the plaquette spins μ_p^z such that it stabilizes the "classical" state of the system.

1.2.2 Conformal quantum critical points

We now turn to the second scenario of perturbing the toric code model via a *wavefunction deformation* that again connects the ground states of the toric code with a fully polarized, paramagnetic state [7, 8]. Along this wavefunction deformation the system goes through a continuous quantum phase transition which is distinct from the one we encountered for the Hamiltonian deformations in the previous section. It belongs in fact to the family of *conformal quantum critical points*, first discussed by Ardonne, Fendley and Fradkin [9], where it is the ground-state wavefunction that becomes *scale invariant*, in a peculiar instance of dimensionality reduction. This in turn allows to describe the *equal-time* correlations in the ground-state wavefunction of a two-dimensional quantum system by those of the related, conformally invariant, *classical* system in 2 dimensions – contrary to the usual correspondence of a D-dimensional quantum system to a $D+1$ dimensional classical system. This dimensionality reduction at a conformal quantum critical point is, of course, reminiscent of the well-known Rokhsar-Kivelson point of the 2D quantum dimer model [13, 14] where in a similar fashion equal-time correlations are captured by a ground-state wavefunction that is the equal-weight superposition of all classical 2D dimer configurations. Following earlier work by Henley [15], Ardonne *et al.* further argued that at a continuous transition, the conformal invariance of the ground state wave function enforces a quantum Lifshitz field theory description, with a characteristic $z = 2$ dynamical exponent [9].

To study wavefunction deformations of the toric code we employ a constructive technique dubbed "stochastic matrix form" decomposition [16] that allows to obtain generalized Rokhsar-Kivelson type Hamiltonians. With this approach we can derive an explicit expression for the ground state wavefunction along the deformation, and we can analyze the intervening conformal quantum critical point in great detail. In particular, we show that the quantum critical behavior is associated with a divergent local length scale, despite the fact that there is no concomitant symmetry breaking phase transition described by a local order parameter. Finally, we turn to entanglement measures and, after a short introduction, we discuss the behavior of the "topological entropy" across the phase transition.

1.2.2.1 Microscopic model for wavefunction deformation

To implement the wavefunction deformation we construct a family of quantum Hamiltonians whose ground states interpolate between the toric code wavefunction (1.1.1) and the fully polarized state $|\psi_p\rangle = \bigotimes_i |\sigma_i^z = +1\rangle$. This can be accomplished by using "stochastic matrix form" (SMF) decompositions [16] for a generic wavefunction of the form

$$|\psi\rangle \propto \sum_{\{\mathbf{s}\,:\,\phi_p(\mathbf{s})=+1\ \forall p\}} \exp\left(\frac{h}{2} E_{\mathbf{s}}\right)\, c_{\mathbf{s}}\, |\mathbf{s}\rangle\,. \tag{1.4}$$

For $h = 0$ this is the toric code ground state, while for $h \to \infty$ the polarized state is exponentially selected, provided that $E_{\mathbf{s}}$ is 'sufficiently peaked' at $\mathbf{s} = \{z_j = +1\}$. The corresponding SMF Hamiltonian can simply be expressed as a sum of projectors that annihilate (1.4). So long as the function(al) $E_{\mathbf{s}}$ can be written as a sum of local terms in the variables $\{z_j\}$, then the Hamiltonian can be constructed as a sum of local operators expressed in terms of the Pauli matrices $\sigma_j^{x,y,z}$.

The simplest example is given by the choice $E_{\mathbf{s}} = \sum_j z_j$. It is straightforward to verify that

$$H = -J_e \sum_s A_s + J_e \sum_s \exp\left(-h \sum_{i\in s} \sigma_i^z\right) \tag{1.5}$$

is a sum of projectors, each of which annihilates (1.4) [16, 7].* However, this remains true if the summation in (1.4) is generalized from $\{\mathbf{s} : \phi_p(\mathbf{s}) = +1\ \forall p\}$ to $\{\mathbf{s} : \phi_p(\mathbf{s}) = \overline{\phi}_p\ \forall p\}$, for any configuration $\{\overline{\phi}_p\}$ of the plaquette eigenvalues. In order to arrive at the desired result, we need to add an appropriate energy cost $-J_m \sum_p B_p$ to the unwanted ground states [7],

$$H = -J_m \sum_p B_p - J_e \sum_s A_s + J_e \sum_s \exp\left(-h \sum_{i\in s} \sigma_i^z\right) \tag{1.6}$$

Not surprisingly, for $h = 0$, the system reduces to the toric code Hamiltonian (1.1), up to a trivial constant shift in energy. Moreover, in the limit $|h| \ll 1$ one can expand the exponential in Eq. (1.6), and to first order one obtains precisely the Hamiltonian deformation studied in the previous section with a longitudinal field $h_z = 2hJ_e$. This equivalence is eventually lost for larger values of h, albeit by construction both models favor indeed the same fully polarized, paramagnetic state for large fields $h \gg 1$.

For convenience of notation, in the following we shall replace the sum over $\{\mathbf{s} : \phi_p(\mathbf{s}) = +1\ \forall p\}$ in Eq. (1.4) in terms of the (Abelian) group G of all spin

*A generic construction scheme for SMF Hamiltonians given arbitrary $E_{\mathbf{s}}$ functionals is provided in Ref. [16].

flip operations obtained as products of star operators A_s [2, 17], so that the ground state wavefunction of model (1.6) reads

$$|\psi_0^{(\alpha)}\rangle = \frac{1}{\sqrt{Z_\alpha}} \sum_{g\in G} \exp\left(\frac{h}{2}\sum_i \sigma_i^z(g,\alpha)\right) g\,|\Psi_\alpha\rangle\,, \tag{1.7}$$

$$\text{with} \quad Z_\alpha = \sum_{g\in G} \exp\left(h\sum_i \sigma_i^z(g,\alpha)\right) \quad \text{and} \quad \sigma_i^z(g,\alpha) \equiv \langle\Psi_\alpha|g\,\sigma_i^z\,g|\Psi_\alpha\rangle.$$

Here the index α labels the 4 topological sectors, i.e., the orbits of the action of the star operators. The eigenstate $|\Psi_\alpha\rangle$ can be chosen arbitrarily amongst the elements of the orbit α, since the action of the group G on any such state generates the entire orbit.

1.2.2.2 Dimensionality reduction and the 2D Ising model

For convenience, we study the quantum phase transition to the paramagnetic state in the topological sector containing the fully polarized state $|\psi_p\rangle = \bigotimes_i |\sigma_i^z = +1\rangle$. The explicit form of the wavefunction reduces to

$$|\psi_0\rangle = \frac{1}{\sqrt{Z}} \sum_{g\in G} \exp\left(h\sum_i \sigma_i^z(g)/2\right) g\;|\psi_p\rangle \quad \text{with} \quad \sigma_i^z(g) \equiv \langle\psi_p|\,g\,\sigma_i^z\,g\,|\psi_p\rangle\;. \tag{1.8}$$

A generic configuration $g\,|\psi_p\rangle$ is uniquely specified by the set of star operators acting on the reference configuration $|\psi_p\rangle$, modulo the action of the product of all the star operators (which is equal to the identity). Thus, there is a 1-to-2 mapping between $G = \{g\}$ and the configuration space $\Theta = \{\boldsymbol{\theta}\}$ of an Ising model with classical degrees of freedom θ_s living on the sites s of the square lattice, where for example $\theta_s = -1$ $(+1)$ means that the corresponding star operator is (not) acting in the associated g. Since each σ-spin can be flipped only by its two neighboring θ-spins, then $\sigma_i \equiv \theta_s\theta_{s'}$, where i labels the bond between the two neighboring sites $\langle s, s'\rangle$. Using this mapping, the ground state wavefunction of the model, Eq. (1.8), can be rewritten as

$$|\psi_0\rangle = \frac{1}{\sqrt{Z}} \sum_{\boldsymbol{\theta}\in\Theta} \exp\left(\frac{h}{2}\sum_{\langle s,s'\rangle} \theta_s\theta_{s'}\right) g(\boldsymbol{\theta})\;|\psi_p\rangle\;, \tag{1.9}$$

where $Z = \sum_{\boldsymbol{\theta}\in\Theta} e^{h\sum_{\langle s,s'\rangle}\theta_s\theta_{s'}}$.

All equal-time correlation functions of the ground state that can be expressed in terms of the classical θ-spins can thus be computed as correlation functions of a $2D$ classical Ising model with reduced nearest-neighbor coupling $J/T = h$ [16]. For small values of the field h, we can identify the equal-time correlation functions of the quantum model in the topological phase with the correlation functions of the high-temperature disordered phase of the 2D Ising

model. Vice versa, the large field paramagnetic state of the quantum model exhibits equal-time correlators that match those of the low-temperature Ising ferromagnetically ordered state. For an intermediate magnetic field strength h_c the ground-state wavefunction of the quantum system becomes "critical" and scale invariant, precisely when the corresponding classical spin system undergoes its thermal phase transition at $h_c = (1/2)\ln(\sqrt{2}+1) \simeq 0.441$.

While the thermal phase transition in the 2D Ising model can be described in terms of a local order parameter, e.g. its magnetization, we note that this is not the case for the original quantum model. For instance, the magnetization in the original σ-spin language translates into the nearest-neighbor spin-spin correlation, i.e., the energy, in the θ-spin language,

$$m(h) = \frac{1}{N}\sum_i \langle\psi_0|\sigma_i^z|\psi_0\rangle = \sum_{\boldsymbol{\theta}\in\Theta} \frac{e^{h\sum_{\langle s,s'\rangle}\theta_s\theta_{s'}}}{Z}\left[\frac{1}{N}\sum_{\langle s,s'\rangle}\theta_s\theta_{s'}\right] = \frac{1}{N}\,E_{\rm Ising}(h)\ ,$$

and one concludes that $m(h)$ does not vanish on either side of the transition. It is continuous across the transition, but there is a singularity in its first derivative

$$\frac{\partial m}{\partial h} = \frac{1}{N}\,\frac{\partial E_{\rm Ising}}{\partial h} = -h^2\ \frac{1}{N}\,C_{\rm Ising}(h)\ , \tag{1.10}$$

as the heat capacity $C_{\rm Ising}(h)$ of the classical Ising model diverges logarithmically at h_c. Thus, while the original quantum model does not allow to define a local order parameter for the phase transition, there is nevertheless a signature of this transition in terms of a singularity in the derivative of a local observable.

1.2.2.3 Topological entropy

We have seen that the unusual properties of topologically ordered phases are inherently linked to non-local properties and a peculiar type of long-range entanglement. With all local correlations being short ranged and non-local correlation functions being tedious to define in more general examples, it is helpful to turn to entanglement measures and to define a *topological entropy* that allows to detect and characterize topological phases [18, 19].

A common measure of quantum entanglement is given by the von Neumann entropy, $S_{\rm vN} = -{\rm Tr}[\rho\ln\rho]$, where ρ is the density matrix of the system. Typically one considers a (smooth) bipartition $(\mathcal{A},\mathcal{B})$ of the system $\mathcal{S} = \mathcal{A}\cup\mathcal{B}$, with boundary size L (which in two dimensions is simply its length), and computes the reduced density matrix $\rho_{\mathcal{A}} = {\rm Tr}_B\rho$. The von Neumann entropy $S_{\rm vN}(\mathcal{A}) = -{\rm Tr}[\rho_{\mathcal{A}}\ln\rho_{\mathcal{A}}]$ is also known as the (bipartite) entanglement entropy, and reflects the 'amount of information' shared between the two subsystems across the boundary. In ordinary short-range correlated phases, the nature of subsystem $\mathcal{B}$ influences subsystem $\mathcal{A}$ only up to some finite distance (of the order of the correlation length) away from the boundary, and

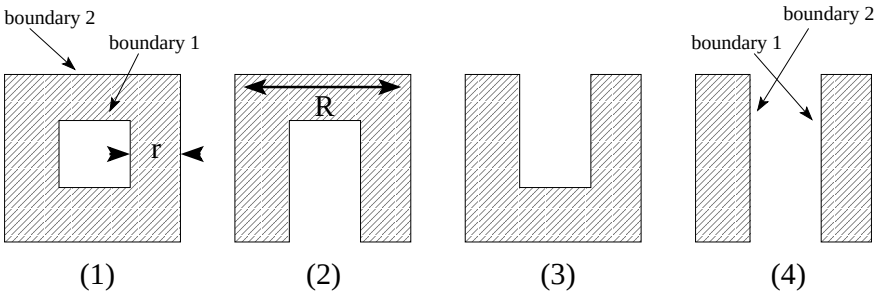

FIGURE 1.5
Bipartition scheme for the topological entropy: Illustration of the four distinct bipartitions $\mathcal{S} = \mathcal{A}_i \cup \mathcal{B}_i$ used to compute the topological entropy in Ref. [18]. The shaded area represents subsystem $\mathcal{A}_i$.

vice versa. To leading order in L the van Neuman entropy thus takes a form $S_{\rm vN}(\mathcal{A}) = \alpha L + \ldots$, where the coefficient α is non-universal.

If, on the other hand, non-local information is stored across a boundary as in the case of a topologically ordered state, it must show up as a further contribution to the entanglement between the two bipartitions $\mathcal{A}$ and $\mathcal{B}$. It was argued in Refs. [17, 18, 19] that this contribution assumes the form of a correction of order one to the previous scaling form, e.g.

$$S_{\rm vN}(\mathcal{A}) = \alpha L - \gamma + O(1/L), \tag{1.11}$$

with all other subleading terms vanishing in the limit $L \to \infty$. This correction $\gamma \geq 0$ is found to be *universal*, and it is related to the so-called "total quantum dimension" of the underlying topological phase [18, 19]. A particularly elegant way to calculate the universal contribution γ is to carefully choose an appropriate set of different bipartitions, such that a linear combination of the respective entanglement entropies cancels out all non-universal terms (at least in the limit of the correlation length being much smaller than the size of the bipartitions). Adopting the scheme proposed in Ref. [18] and illustrated in Fig. 1.5, we define the topological entropy as:

$$S_{\rm topo} = \lim_{r,R\to\infty} \Big[- S_{\rm vN}(\mathcal{A}_1) + S_{\rm vN}(\mathcal{A}_2) + S_{\rm vN}(\mathcal{A}_3) - S_{\rm vN}(\mathcal{A}_4) \Big], \tag{1.12}$$

where the indices $i = 1, \ldots, 4$ label the four different bipartitions $\mathcal{S} = \mathcal{A}_i \cup \mathcal{B}_i$. Note that bipartitions $(\mathcal{A}_1, \mathcal{B}_1)$ and $(\mathcal{A}_4, \mathcal{B}_4)$ combined have the same total boundary, with the same number and type of corners, as bipartitions $(\mathcal{A}_2, \mathcal{B}_2)$ and $(\mathcal{A}_3, \mathcal{B}_3)$ combined. As a result, the non-universal part of the entanglement entropy due to local correlations cancels out in Eq. (1.12). However, only bipartitions $(\mathcal{A}_1, \mathcal{B}_1)$ and $(\mathcal{A}_4, \mathcal{B}_4)$ are topologically non-trivial, and the universal correction to the corresponding entanglement entropies is doubled. This definition of $S_{\rm topo}$ therefore measures twice the value of γ, i.e., $S_{\rm topo} = 2\gamma$.

Any approach to compute the topological entropy faces the challenge of isolating a subleading term of order one in a quantity, the entanglement entropy, that scales with the size L of the bipartition. (This, of courses, raises the question whether there are better measures of the long-range entanglement of topological phases.) Perturbative techniques can be used only if the achieved accuracy is greater than $O(1/L)$. Likewise, it is rather difficult to obtain reliable numerical estimates [20]. On the other hand, at zero temperature the density matrix of the system becomes the projector onto the ground state $|\psi_0\rangle$, namely $\rho = |\psi_0\rangle\langle\psi_0|$, and one can attempt to calculate $S_{\rm vN}$ and $S_{\rm topo}$ directly whenever an explicit expression for the ground state wavefunction is available. Hereafter, we follow this approach and compute the topological entropy for the "wavefunction deformation" of the toric code presented in Sec. 1.2.2.1.

1.2.2.4 Topological entropy along the wavefunction deformation

To calculate the topological entropy along the wavefunction deformation we consider a smooth bipartition $(\mathcal{A}, \mathcal{B})$ of the system. Let us define the subgroup $G_{\mathcal{A}} \subset G$ that acts solely on $\mathcal{A}$ and leaves $\mathcal{B}$ invariant: $G_{\mathcal{A}} = \{g = g_{\mathcal{A}} \otimes g_{\mathcal{B}} \in G \mid g_{\mathcal{B}} = \mathbf{1}_{\mathcal{B}}\}$. Likewise we define $G_{\mathcal{B}}$. Following Ref. [7] the von Neumann entropy $S_{\rm vN}(\mathcal{A})$ from the ground state wavefunction in Eq. (1.8) can be expressed as

$$S_{\rm vN}(A) = -\frac{1}{Z}\sum_{g\in G} e^{-hE_g}\ \ln\left(\frac{1}{Z}\sum_{f\in G_A,\, k\in G_B} e^{-hE_{fgk}}\right), \qquad (1.13)$$

where $E_g = -\sum_i \sigma_i^z(g)$. This is the lattice equivalent of the von Neumann entropy obtained by Fradkin and Moore for quantum Lifshitz field theories [21]. Note that this expression for the von Neumann entropy can also be interpreted as the "entropy of mixing" (or configurational entropy) of the allowed boundary configurations in G (this was first shown in Ref. [7], and later investigated in more detail in Ref. [22]).

Employing the change of variables to classical Ising degrees of freedom $\{\theta_s\}$ (see Sec. 1.2.2.2), and omitting the technical details [7] required to deal with configurations of the form fgk ($f \in G_A$ and $k \in G_B$), one can use Eq. (1.13) to obtain the topological entropy of the system as a function of h (with the bipartition scheme illustrated in Fig. 1.5)

$$S_{\rm topo} = \lim_{r,R\to\infty}\left\{\frac{\sum_{g\in G} e^{-hE_g}}{Z} \times \ln\frac{\left[Z_1^{\partial}(g) + Z_1^{\partial,\,\rm twisted}(g)\right]\left[Z_4^{\partial}(g) + Z_4^{\partial,\,\rm twisted}(g)\right]}{Z_2^{\partial}(g) Z_3^{\partial}(g)}\right\}. \qquad (1.14)$$

Here $Z_2^\partial(g)$ and $Z_3^\partial(g)$ represent the partition functions of an Ising model with nearest-neighbor interactions of reduced strength $J/T = h$, and with fixed spins along the boundary of bipartitions 2 and 3, respectively. Likewise, $Z_{1,4}^\partial(g)$ are analogous partition functions for bipartitions 1 and 4, respectively. Note that the boundaries in bipartitions 1 and 4 have two disconnected components, labeled 'boundary 1' and 'boundary 2' in Fig. 1.5. The partition functions $Z_{1,4}^{\partial,\,\mathrm{twisted}}(g)$ differ from $Z_{1,4}^\partial(g)$ in that all the (fixed) spins belonging to boundary 2 in bipartitions 1 and 4, respectively, have been flipped.

The sum over g in Eq. (1.14) acts as a weighed average of the logarithmic term over all possible values of the spins at the boundary. Notice that the partitions with two boundaries, and hence with non-trivial topology, are those that appear with two contributions (bipartitions 1 and 4), corresponding to the sum of each boundary condition with its twisted counterpart.

In the topological phase (i.e., in the disordered phase of the corresponding Ising model), where correlations are short ranged, the choice of boundary conditions affects the partition function of the system only with exponentially small corrections. Thus, we can expect to have $Z_1^\partial(g)Z_4^\partial(g) \simeq Z_1^{\partial,\,\mathrm{twisted}}(g)Z_4^\partial(g) \simeq \ldots \simeq Z_2^\partial(g)Z_3^\partial(g)$ and the topological entropy becomes $S_{\mathrm{topo}} = \ln 4$. On the other hand, in the polarized paramagnetic phase (i.e., in the ferromagnetically ordered phase of the Ising model) the partition function of a system with twisted boundary conditions is exponentially suppressed with respect to the one without the twist. Thus, $Z_1^\partial(g) \gg Z_1^{\partial,\,\mathrm{twisted}}(g)$, $Z_4^\partial(g) \gg Z_4^{\partial,\,\mathrm{twisted}}(g)$, while $Z_1^\partial(g)Z_4^\partial(g) \simeq Z_2^\partial(g)Z_3^\partial(g)$ still holds. This leads to $S_{\mathrm{topo}} = 0$.

Using a high-temperature expansion for $h < h_c$, and appropriate Ising duality relations for $h > h_c$, one can show that the behavior of the topological entropy across the transition is *discontinuous*, with a sudden jump from $S_{\mathrm{topo}} = \ln 4$ to $S_{\mathrm{topo}} = 0$ at h_c, in spite of the otherwise continuous nature of the transition [7]. This discontinuity of the topological entropy is probably less surprising if one keeps in mind that the topological entropy is inherently linked to the quantum dimensions of the elementary excitations of a phase [18, 19], and thus it must remain constant for the full extent of the phase.[†]

1.3 Thermal transitions

Our discussion so far was from a purely zero temperature perspective of phase transitions involving topologically ordered phases. In conventional quantum

[†]A similar behavior of the topological entropy has been found in numerical simulations [23] of the Hamiltonian deformation discussed in section 1.2.1.

phase transitions – where a local order parameter acquires a non-vanishing expectation value – the zero-temperature quantum critical point controls an extended portion of the finite temperature phase diagram, the so-called "quantum critical region" or "quantum critical fan". One thus wonders to what extent a similar behavior can be expected to hold for quantum phase transitions involving topological phases of matter. To address this question, we first discuss a framework to measure and characterize topological order at finite temperature, using both non-local correlators and a generalization of the topological entropy. This will further allow to discuss when topological order survives in the presence of thermal fluctuations, and under what conditions one can expect to observe a *finite-temperature* phase transition.

1.3.1 Non-local order parameters at finite temperature

At zero temperature we can typically characterize topological order by non-local order parameters, for instance the winding loop operators in the toric code [2]. If we want to use the same order parameters at *finite* temperature, one needs to carefully consider the role of defects, e.g. a flipped spin occurring along the path of a winding loop operator, which changes its expectation value. In a topological phase with excitation gap Δ, a finite temperature T induces a finite density $\rho \sim e^{-\Delta/T}$ of defects. Our ability to 'detect' the topological phase using loop operators relies on the ability to find loops that do not encounter any thermal defects along their path. However, the probability for the occurrence of such unaffected loops scales as $(1-\rho)^\ell$, where ℓ is the total length of the loop. For winding loops with $\ell \geq L$, where L is the linear size of the system, this probability vanishes exponentially fast in the thermodynamic limit – irrespective of how low the temperature is. This phenomenon was first discussed in the context of topological phases in Ref. [24] and termed "thermal fragility".[‡] This is quite distinct from conventionally ordered phases, where the thermal uncertainty in the expectation value of a local order parameter scales with the density of defects, and becomes negligibly small at low temperature.

Note that this thermal fragility of non-local order parameters cannot directly be equated to a thermal instability of the topological phase. The latter is determined by the nature of the anyonic defects, and stable topological phases at finite temperature are indeed possible [26], which can be captured by the behavior of the topological entropy of the system [27].

For a *finite* system one can nevertheless define a *crossover temperature* T^*. The free energy of a pair of defects, each with gap Δ, is $F = 2\Delta - T\ln N(N-1) \sim 2\Delta - 2T\ln N$. Above a temperature $T^* = \Delta/\ln N$ we always encounter excitations, but for $T \ll T^* \sim 1/\ln N$ the system is protected. This

[‡]The reader familiar with the connection between toric code and $\mathbb{Z}_2$ lattice gauge theory may recognize that this statement follows from the property that the expectation value of Wilson loop operators always vanishes in the limit of infinite loop size [25].

logarithmic reduction of the gap scale is no major technological problem for potential future devices built on such phases that might operate on system sizes $N \sim 100$. It is, however, an interesting and important aspect when discussing topological stability.

1.3.2 Topological entropy at finite temperature

To characterize the stability of a topological phase at finite temperature we now turn to topological entropy. While entanglement entropies are often considered zero-temperature quantities, we can readily generalize their definition in terms of the density matrix to finite temperature by simply considering $\rho(T) = \exp(-\beta H)/\mathrm{Tr}[\exp(-\beta H)]$, where H is the Hamiltonian and $\beta = 1/k_B T$.

Computing the so-generalized topological entropy S_{topo} at finite temperature often turns out to be a significant challenge, even for state of the art numerical techniques [20]. On the other hand, some instances such as the toric code model are simple enough to allow for a rigorous calculation as a function of both system size and temperature [28, 27, 29], as we briefly discuss in the following.

In the toric code Hamiltonian (1.1) we have seen that plaquette (P) and star (S) operators commute with one another. When calculating the finite-temperature generalizations of the entanglement and topological entropies, the resulting expressions are additive in these two contributions

$$S(\mathcal{A}; T) = S^{(P)}(\mathcal{A}; T/J_m) + S^{(S)}(\mathcal{A}; T/J_e)\,. \tag{1.15}$$

Therefore, vortex defects, i.e. plaquette operators with negative eigenvalues, are immaterial to the star contribution and vice versa. As a consequence, one can conveniently consider the two contributions separately. Moreover, the system is symmetric upon exhanging x with z spin components, and plaquettes with stars. The two contributions $S^{(P)}$ and $S^{(S)}$ can thus be cast in the exact same analytical form.

Deriving the explicit expressions for $S^{(P)}_{\mathrm{topo}}(T/J_m)$ and $S^{(S)}_{\mathrm{topo}}(T/J_e)$ as a function of temperature and system size N is a rather cumbersome exercise and we refer to Ref. [28] for a detailed description. In both cases temperature and system size enter these expressions through the product $\mathcal{K}_{e,m} = N \ln[\coth(J_{e,m}/T)]$, respectively. Hence, the thermodynamic limit, $N \to \infty$, and the zero temperature limit, $T \to 0$, do not commute. The zero-temperature value of the topological entropy, $S_{\mathrm{topo}} = \ln 4$, is recovered *only* if the temperature is lowered to zero whilst keeping the system size finite. Vice versa, in the thermodynamic limit the topological entropy vanishes at any finite T, no matter how small.

In Fig. 1.6 we plot the analytical expressions for the topological entropies $S^{(P)}_{\mathrm{topo}}(T/J_m)$ and $S^{(S)}_{\mathrm{topo}}(T/J_e)$ as a function of $\mathcal{K}_{e,m}$. For a fixed system size N, the plotted behavior indicates that the topological entropy decays to zero

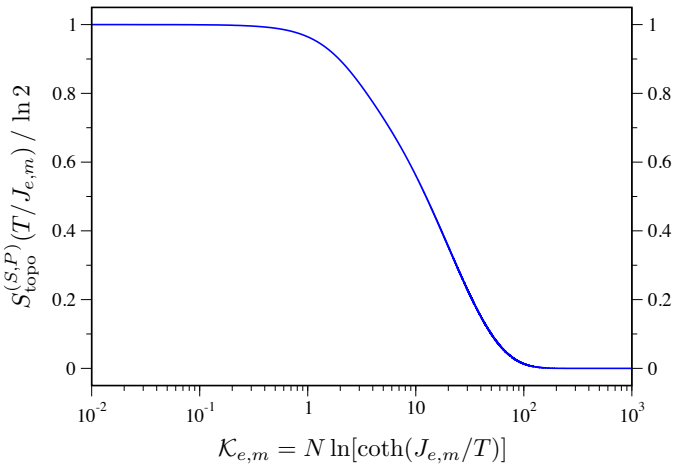

FIGURE 1.6
Finite-temperature topological entropy of the toric code: $S_{\rm topo}^{(S,P)}(T/J_{e,m})$ as a function of $\mathcal{K}_{e,m} = N\ln[\coth(J_{e,m}/T)]$.

at a finite temperature. With $T \ll J_{e,m}$ we can expand $N\ln[\coth(J_{e,m}/T)] \sim 2N\exp(-2J_{e,m}/T)$, where the exponential corresponds to the Boltzmann weight for a single spin flip to occur in the ground state of the system, i.e., the density of defects. The decay in Fig. 1.6 occurs when $N\exp(-2J_{e,m}/T) \sim 1$, that is when the average *number* of defect pairs in the system is of order unity. This translates into a crossover temperature $T^* \sim 2J_{e,m}/\ln N$, in agreement with the behavior of the non-local order parameters discussed earlier.

1.3.3 Fragile vs robust behavior: a matter of (de)confinement

The results in Sec. 1.3.2 and Sec. 1.3.1 show that the topological order in the 2D toric code is truly fragile to thermal fluctuations, in the sense that it is destroyed by a finite *number* of defects. In the thermodynamic limit there is no finite-temperature phase transition.

From the behavior of the non-local operators one might *mistakenly* conclude that this fragility to thermal fluctuations is intrinsic to topological order [24]. On the other hand, we can compare this to the well-known example of a classical Z_2 lattice gauge theory in three dimensions [3, 30], which also lacks a local order parameter in the zero temperature limit. There, the $T = 0$ state does not subside immediately to thermal fluctuations, and a finite temperature phase transition exists between a low-temperature phase with confined defects, and a high-temperature phase where the defects are deconfined (see also Sec. 1.2.1). Whereas non-local operators (such as Wilson loops around the whole system) vanish in both phases in the thermodynamic limit, the fi-

nite temperature phase transition is ultimately captured by the way that the winding loop expectation values vanish as the system size is increased (the area vs. perimeter law [25]).

Key to the existence of a finite temperature phase transition in the Z_2 lattice gauge theory is the confined nature of the thermal excitations in the low-temperature phase. Consistently, the deconfined nature of the defects in the topological phase of the toric code in two dimensions leads to the observed fragile behavior at finite temperature. If, on the other hand, we can devise a model where the excitations are confined, then we might expect a qualitatively different behavior. One example of the latter is the three-dimensional generalization of the toric code [31]. In this model, plaquette and star operators are no longer dual to each other, and while the star defects give rise to point-like excitations – much like in the 2D case – plaquette defects become objects which define closed loops (through plaquettes where the stabilizer condition of the ground states is violated), whose energy cost scales with the length of the loop. As a consequence, the plaquette defects do not fractionalize, but rather form confined structures whose characteristic size is controlled by temperature [26]. This low-temperature phase with confined plaquette excitations is therefore stable to thermal fluctuations resulting in a finite-temperature (continuous) phase transition at $T_c/J_{m,e} \simeq 1.313346(3)$ [27]. While the star contribution to the topological entropy exhibits a fragile behavior (just as in the two-dimensional case), the plaquette contribution survives unaltered up to the finite-temperature phase transition [27].

These results illustrate that the robustness of a zero-temperature topological phase depends crucially on the confined versus deconfined nature of the thermal excitations. Only if *all* excitations are confined, we expect quantum topological order to survive up to a finite temperature phase transition [26].

1.4 Outlook

In this chapter we discussed phase transitions involving topologically ordered phases of matter in deformations of the toric code model. We focused on continuous quantum critical points where appropriate local correlators exhibit a divergent behavior. We showed that the growing correlations characterizing the critical region can be understood in terms of 'dual' degrees of freedom, which undergo a conventional quantum phase transition between a disordered phase (corresponding to the topologically ordered one in the original system), and an ordered one characterized by a local order parameter (in the dual degrees of freedom). In this dual language, the underlying topological order is typically invisible – the topological degeneracy being "mapped out" by the many-to-one correspondence in the definition of the dual degrees of freedom

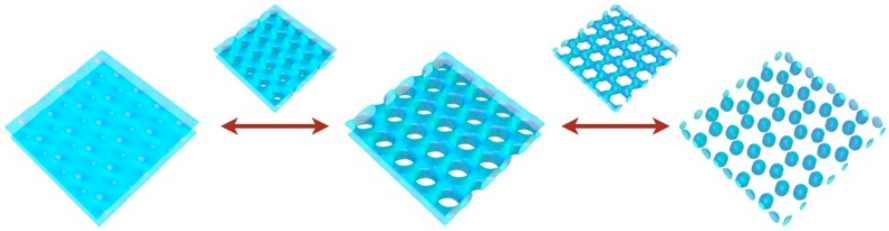

FIGURE 1.7
Topology driven quantum phase transition: Two-dimensional surfaces with different topologies that are populated by anyonic quantum liquids. A quantum phase transition driven by fluctuations of the surface topology connects the anyonic liquid with topological order on two separated sheets (on the left) and the anyonic liquid without topological order on decoupled spheres (on the right).

(see in particular the discussion in Sec. 1.2.2.2 and Ref. [32]). Indeed, while the disruption of topological order across the transition occurs *because of* the conventional phase transition in the underlying dual system, topological order survives unaffected up to the critical point (as whitnessed for instance by the step-function behavior of the topological entropy), irrespective of the continuous vs first-order nature of the transition (see Sec. 1.2.1.1). The two phenomena – the change in topological properties and the underlying conventional phase transition – appear to be essentially unrelated in nature.

One is then left to wonder whether it would be possible for a perturbation to cause topological order to subside or change *without signature in any local correlators*. Such transitions could take place either between topologically ordered phases, or between a topologically ordered phase and a conventional paramagnet, somewhat akin to a glass transition in classical systems. Contrary to the examples considered in this chapter, these transitions would be detected *exclusively* by non-local observables. Or is it the case that even when there is no local order parameter on either side of the transition (whether in the original or dual degrees of freedom), there *must* generically be a detectable singularity in high enough derivatives of some local observables? One approach that does not require any *a priori* knowledge of an order parameter, and which has been argued to detect any singularities in local observables, has recently been proposed by Zanardi *et al.* based on the information theoretic concept of fidelity [33]. [§] However, it remains to be seen whether fidelity-based techniques can be applied in systems where more conventional approaches fail.

[§]Examples of fidelity-based approaches to characterize quantum phase transitions involving topologically ordered phases of matter can be found for instance in Refs. [23, 34].

Another open question is whether the usual picture of a "fan"-like quantum critical region in the finite temperature phase diagram above a quantum critical point [35] also applies to quantum phase transitions involving topological order. Does such a fan exist only in the presence of local order parameters, either in the system at hand or a dual description, as was the case for the toric code and its dual description in terms of an Ising model? Or does a similar phenomenon appear at all continuous quantum phase transitions out of topological phases? A first attempt at addressing this question was recently made by Chung *et al.* in Ref. [36], where a quantum phase transition separating an Abelian from a non-Abelian topological phase was investigated in the context of an exactly solvable chiral spin liquid model. What Chung *et al.* showed is how non-local order parameters can be used to define a crossover temperature T^* – akin to the one discussed in Sec. 1.3.1 – which thereby allows to define a temperature region reminiscent of the quantum critical fan in systems with local order parameters. The precise nature of this region, and whether its physics is as rich as for conventional quantum phase transitions, remains however an open question.

More generally, we still need to identify a unifying theoretical framework that allows to describe topological phases and their phase transitions – akin to the Landau-Ginzburg-Wilson theory for conventional quantum phase transitions. A step towards such a more general description was taken in Ref. [37] where the field-driven quantum phase transition in the toric code model was described in terms of a mutual Chern-Simons Landau-Ginzburg theory. However, a generalization of this approach to non-Abelian phases is non-trivial.

A unifying framework to describe quantum phase transitions for both Abelian and non-Abelian topological phases has recently been proposed by some of us by considering a general description in terms of quantum double models [38]. An Abelian or non-Abelian topological phase in a time-reversal invariant quantum lattice model, such as the toric code or the Levin-Wen model [39], can be constructed from *chiral* topological quantum liquids populating the closed surface geometry obtained by "fattening" the edges of the lattice model, as illustrated for a honeycomb lattice in the middle panel of Fig. 1.7. In this picture the quantum phase transition going from a topologically ordered phase to a (topologically trivial) paramagnetic state then corresponds to the transition between different surface topologies as shown in Fig. 1.7. The topological phase corresponds to the limit of "two sheets" illustrated on the left, while the paramagnet corresponds to the limit of "decoupled spheres" illustrated on the right. Plaquette flux excitations in the lattice model correspond to "wormholes" in the quantum double model connecting the two sheets. Independent of their braiding statistics it is the proliferation of these wormholes that drives a quantum phase transition between the two extremal states. The critical point between the topological and trivial phases is then described by a "quantum foam" where the *surface topology fluctuates* on all length scales. This concept of a "topology-driven quantum phase transition" thereby provides a general framework that describes the quan-

tum critical behavior of time-reversal invariant systems exhibiting topological order.

Acknowledgments

S.T. and M.T. thank the Aspen Center for Physics for hospitality. C.C.'s work was supported by the EPSRC Grant No. GR/R83712/01 and by the EPSRC Postdoctoral Research Fellowship EP/G049394/1. We thank E. Ardonne, C. Chamon, and E. Kim for carefully reading the manuscript. C.C. is particularly grateful to C. Chamon for stimulating discussions which led to some of the ideas presented in the Outlook section.

References

[1] X.-G. Wen, Phys. Rev. B **40**, 7387 (1989).

[2] A. Y. Kitaev, Ann. Phys. (N.Y.) **303**, 2 (2003).

[3] J. B. Kogut, Rev. Mod. Phys. **51**, 659 (1979).

[4] S. Trebst, P. Werner, M. Troyer, K. Shtengel, and C. Nayak, Phys. Rev. Lett. **98**, 070602 (2007).

[5] I. S. Tupitsyn, A. Kitaev, N. V. Prokof'ev, P. C. E. Stamp, arXiv:0804.3175.

[6] J. Vidal, S. Dusuel, K. P. Schmidt, Phys. Rev. B **79**, 033109 (2009).

[7] C. Castelnovo and C. Chamon, Phys. Rev. B **77**, 054433 (2008).

[8] S. Papanikolaou, K. S. Raman, and E. Fradkin, Phys. Rev. B **76**, 224421 (2007).

[9] E. Ardonne, P. Fendley, and E. Fradkin, Ann. Phys. (N.Y.) **310**, 493 (2004).

[10] E. Fradkin and S. Shenker, Phys. Rev. D **19**, 3682 (1979).

[11] H.W. J.Blöte and Y. Deng, Phys. Rev. E **66**, 066110 (2002).

[12] J. Vidal, R. Thomale, K. P. Schmidt, S. Dusuel, Phys. Rev. B **80**, 081104 (2009).

[13] D. Rokhsar and S. Kivelson, Phys. Rev. Lett. **61**, 2376 (1988).

[14] C. L. Henley, J. Phys.: Condens. Matter **16**, S891 (2004).

[15] C. L. Henley, J. Stat. Phys. **89**, 483 (1997).

[16] C. Castelnovo, C. Chamon, C. Mudry, and P. Pujol, Ann. Phys. (N.Y.) **318**, 316 (2005).

[17] A. Hamma, R. Ionicioiu, and P. Zanardi, Phys. Rev. A **71**, 022315 (2005); Phys. Lett. A **337**, 22 (2005).

[18] M. Levin, and X.-G. Wen, Phys. Rev. Lett. **96**, 110405 (2006).

[19] A. Y. Kitaev, and J. Preskill, Phys. Rev. Lett. **96**, 110404 (2006).

[20] S. Furukawa and G. Misguich, Phys. Rev. B **75**, 214407 (2007).

[21] E. Fradkin, and J. E. Moore, Phys. Rev. Lett. **97**, 050404 (2006).

[22] J.-M. Stéphan, S. Furukawa, G. Misguich, and V. Pasquier, Phys. Rev. B **80**, 184421 (2009).

[23] A. Hamma, W. Zhang, S. Haas, and D. A. Lidar, Phys. Rev. B **77**, 155111 (2008).

[24] Z. Nussinov and G. Ortiz, PNAS **106**, 16944 (2009); Ann. Phys. (N.Y.) **324**, 977 (2009).

[25] F. J. Wegner, J. Math. Phys. **12**, 2259 (1971).

[26] E. Dennis, A. Kitaev, A. Landahl, and J. Preskill, J. Math. Phys. **43**, 4452 (2002).

[27] C. Castelnovo and C. Chamon, Phys. Rev. B **78**, 155120 (2008).

[28] C. Castelnovo and C. Chamon, Phys. Rev. B **76**, 184442 (2007).

[29] C. Castelnovo and C. Chamon, Phys. Rev. B **76**, 174416 (2007).

[30] K. G. Wilson, Phys. Rev. D **10**, 2445 (1974); R. Balian, J. M. Drouffe, and C. Itzykson, Phys. Rev. D **11**, 2098 (1975); E. Fradkin and L. Susskind, Phys. Rev. D **17**, 2637 (1978); E. Fradkin and S. Raby, Phys. Rev. D **20**, 2566 (1979); L. Susskind, Phys. Rev. D **20**, 2610 (1979).

[31] A. Hamma, P. Zanardi, and X.-G. Wen, Phys. Rev. B **72**, 035307 (2005).

[32] X-Y. Feng, G.-M. Zhang, and T. Xiang, Phys. Rev. Lett. **98**, 087204 (2007).

[33] P. Zanardi, L. Campos Venuti, P. Giorda, Phys. Rev. A**76**, 062318 (2007), and references therein.

[34] E. Eriksson and H. Johannesson, Phys. Rev. A. **79**, 060301(R) (2009).

[35] S. Chakravarty, B. I. Halperin, and D. R. Nelson, Phys. Rev. B **39**, 2344 (1989).

[36] S. B. Chung, H. Yao, T. L. Hughes, and E.-A. Kim, arXiv:0909.2655.

[37] S. P. Kou, J. Yu, and X.G. Wen, Phys. Rev. B **80**, 125101 (2009).

[38] C. Gils, S. Trebst, A. Kitaev, A. W. W. Ludwig, M. Troyer, and Z. Wang, Nature Physics **5**, 834, (2009).

[39] M. Levin, and X.-G. Wen, Phys. Rev. B **71**, 045110 (2005).